ASIAN JOURNAL OF CIVIL ENGINEERING (BHRC) VOL. 16, NO. 8 (2015)
PAGES 1089-1101

# SEISMIC VULNERABILITY ASSESSMENT OF REINFORCED CONCRETE STRUCTURE IN TABRIZ NORTH FAULT VICINITY

A. Irani* and A. Jalali
Engineering Faculty of Tabriz University

**Received:** 12 March 2015; **Accepted:** 23 June 2015

## ABSTRACT

The aim of this paper is determining the probability of seismic vulnerability of two building, 8 and 5 storied, reinforced concrete residential building as examples of existing buildings in high risk area, in Tabriz. These structures have been modeled in 3D frame in SAP2000 software [17] and excitation with selected twenty ground motion records. Each record have 15 synthetic records. As a result, a total of 300 records were entered into SAP2000. We evaluate the ISDR at each storey and retain the maximum value to give an overall idea of the building damage level.
By comparing structures response together and with damage states, it can be concluded that the structures reach to initially predicted performance. The study presented in this article summarizes the vulnerability analysis for the case studies of Tabriz in East Azerbaijan (the north-west of Iran). These buildings are of regular shape with 8 and 5 numbers of stories. The analysis consider seven damage states, from none to complete collapse, complying with Rossetto and Elnashai [15] classification.

**Keywords:** Seismic Vulnerability, Fragility Curves, Damage States, Near Fault, ISDR.

## 1. INTRODUCTION

Iran is located at the Alps - Himalaya earthquake belt and this part of the world is an active earthquake zones. The occurrence of large earthquakes, whit large magnitude about four every four days and also mordant experience of destructive earthquakes in recent years, the necessity and importance in earthquake engineering studies reveals.

In particular, there isn't the fragility curves of local earthquake in this area and the construction of residential buildings are not according to the popular construction standards, despite the relatively good design principles. These reasons show the importance of further studying about earthquake.

Therefore, providing the fragility curves for representatives of typical residential

*E-mail address of the corresponding author: alirezairany@gmail.com (A. Irani)

buildings, designed and built in this area, is the main objective of the present study. Although Residential buildings built in the area includes a wide range. But a quick checking show that major class of buildings are intermediate moment concrete frame structures without shear wall and with infill. The elevation of most buildings in the area is observed between 5 and 10 stories.

To investigate the structure behavior, they have been excited by great earthquake occurred and registered throughout the world. Causative fault of these earthquake and other site conditions have been matched by selected cases. In this study vulnerability function assessments are doing based on Rossetto and Elnashai [15, 16] studies for European and similar seismic risk assessment scenario. They present a method wherein data for different structural systems can be combined to produce a single set of 'homogenised' or 'general' curves applicable to all, through the use of a damage scale that accounts for the differences in the damage rate of disparate systems and experimental data used in the calibration of FEMA-273 is limited to tests on low rise concrete shear walls, new RC structures and non-structural elements published in Kircher et al. [12], Ferritto [5], and Division of the State Architect Report [2], respectively.

## 2. METHOD AND MATERIALS

The major aim of this study is development of fragility curves for concrete structures in near fault region, Tabriz, Iran. To this end, the structures analyse nonlinear dynamic time history by using of SAP2000 computer software. Obtained results used to probability calculation by coding with Compaq Visual FORTRAN Ver.6 and fragility curves developing.

The case studies are two building with 5 and 8 number of stories located in Tabriz. East Azerbaijan. Iran. This city in North-West of Iran is in region of intense deformation and seismicity, situated between two thrust belts of the Caucasus to the north and the Zagros Mountains to the south [7]. In this region, North Tabriz Fault which has a well-known history of intense seismic activity is passing through in close distance of urban area (Near field effect on horizontal equal-hazard spectrum of Tabriz city in north-west of Iran [19].

Selection of structures was based on Experiences of the author at residential buildings construction in this region. These building structures are intermediate moment concrete frame. 8 stories building has joist floors, two level parking stories, one underground stories, parking ramp and opening on first floor and don't has shear wall. 5 stories building has joist floors, one level parking storey, one pent house storey and doesn't have shear wall. Both buildings have cantilever in south view. Simulated 3D models are shown in Fig. 1. Section properties of structure beam and column elements presented in Table. 1.

Table 1: Column and Beam Section of case study buildings

| Story | Element | Dim. | Element | Dim. |
|---|---|---|---|---|
| 5-Storey Building | | | | |
| 1 & 2 | Column | 45 × 45 | Beam | 45 × 35<br>45 × 25 |
| 3 & 4 | Column | 40 × 40 | Beam | 45 × 30 |

| | | | | |
|---|---|---|---|---|
| Pent | Column | 35 × 35<br>40 × 40 | Beam | 45 × 25<br>40 × 30<br>35 × 25 |
| | | 8-Storey Building | | |
| 1 & 2 | Column | 65 × 65 | Beam | 60 × 40<br>50 × 40<br>60 × 50 |
| 3 & 4 | Column | 60 × 60 | Beam | 60 × 40<br>50 × 40<br>60 × 50 |
| 5 & 6 | Column | 55 × 55 | Beam | 60 × 40<br>50 × 40<br>60 × 50 |
| 7 | Column | 50 × 50 | Beam | 60 × 40<br>50 × 40<br>60 × 50 |
| 8 | Column | 45 × 45 | Beam | 60 × 40<br>50 × 40<br>60 × 50 |

These case studies designed with both the Iranian Standard No. 519 (2000), 2800 (3rd Edition, 2005) and Iranian Concrete Structures (ABA) Code (2nd Edition, 1998). The structures design by Etabs2000 software and earthquake force calculated with equivalent static method. Control criteria states of structure design are done.

The main problem with designing earthquake resistant RC buildings is defining the anticipated forces and providing for these by proper proportioning and detailing of members. The general approach of engineers to design a structure consists of determining the expected demands and providing the necessary capacity to meet the demands. In earthquake resistant design, it is more complicated to estimate appropriate design loads due to the uncertainty that surrounds them [3].

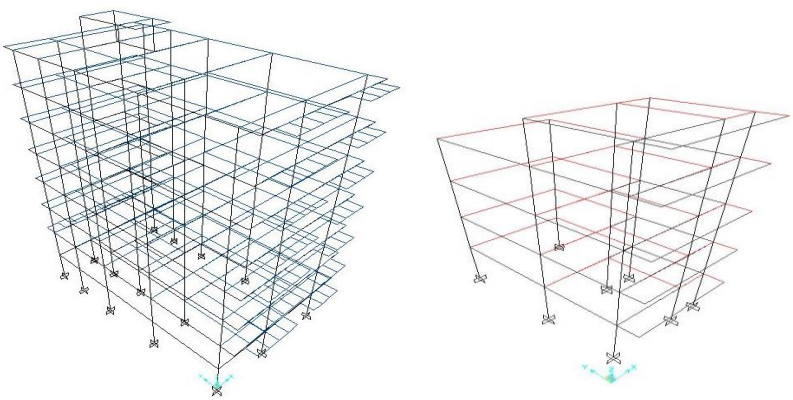

Figure 1. Simulated 3D Model of 5 and 8 Stories Building

Ground motion databases are selected after investigation of case studies site conditions. These records used as input data for dynamic time history analysis in SAP2000 software. Tabriz region in north-western of Iran as a part of the Alpine- Himalayan belt is in between the Arabian Shield in the southwest and the Eurasia plate in the north-east. Earthquake focal mechanisms indicate faults in region mainly are WNW trending right-lateral strike-slip. The North Tabriz Fault is the most prominent tectonic structure in the immediate vicinity of Tabriz city with right lateral fault mechanism [8]. An assessment of seismic collapse risk shows that the predicted probability of collapse in 50 years for modern concrete buildings at a representative near-fault site is approximately 6%, which is significantly higher than the 1% probability in the far-field region targeted by current seismic design maps in the U.S. [13].

In the near-fault region, ground motions sometimes exhibit a large pulse near the beginning of the velocity time history. These pulse-like ground motions may occur at near-fault sites when the fault rupture propagates toward the site and the rupture velocity is similar to the shear wave velocity, leading to constructive interference of the wave front and the arrival of the seismic energy from the rupture in a large amplitude pulse [6]. The near-field of an earthquake (also called near-source or near-fault region) is the region within which distinct pulse-like particle motions are observed due to a coherent release and propagation of energy from the fault rupture process. For damaging earthquakes, the near-field region may extend several kilometres outward from the projection on the ground surface of the fault rupture zone and its extension to the surface, particularly in the direction of rupture propagation [9]. fault-normal/fault-parallel (FN/FP) directions is important in designing of structures that are in near fault region, for this reason in new building codes recommended combination methods for both direction effects [11].

10 to 20 ground motion databases give acceptable accuracy in seismic demand estimate [20]. As mentioned above, for the ground motion selection criteria, 20 earthquake ground motions records are selected satisfying the following conditions:

- Ground motions records having strike-slip faulting mechanism
- Ground motions records having distance from 0 to 10 km
- Ground motions records are horizontal directions

All of the earthquake ground motions are downloaded from strong motion Databases of PEER (http://peer.berkeley.edu/smcat/) [14]. All records have been downloaded in august 2014. Two sample of this near fault records presents in Fig.2. 20 earthquake records and their properties are summarized in Table 2.

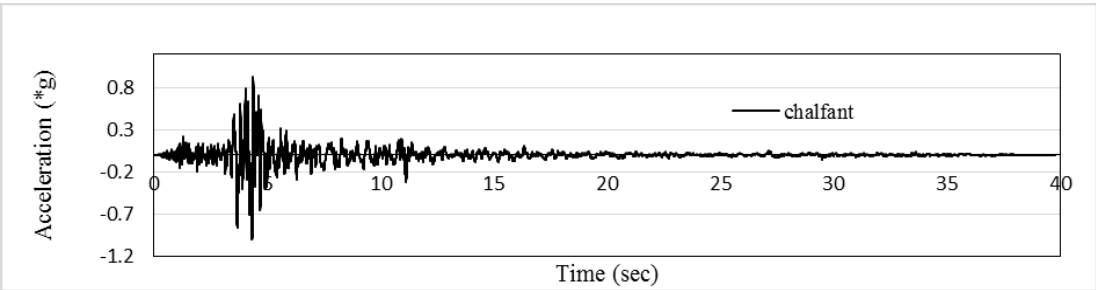

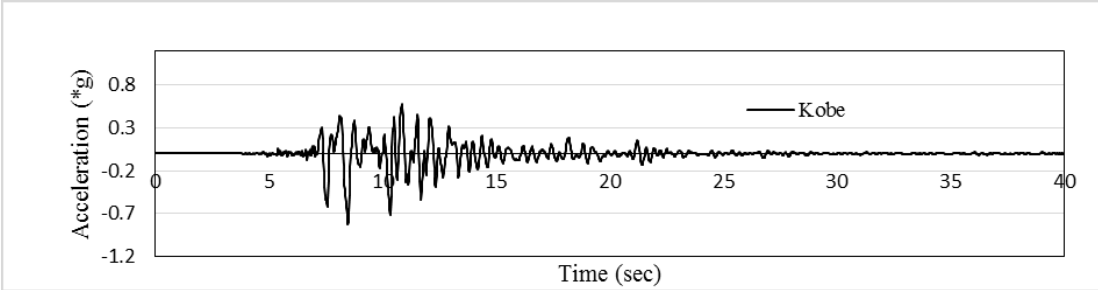


Figure 2. Acceleration time history of Chalfant Valley 1986, 54171 Bishop St. and Kobe 1995, KJMA St

At first all records normalized with self PGA value. Hence acceleration values will be 0 to 1. Then acceleration values multiply to 0.1g, 0.2g, …, 1.5g thus we have 300 numbers of record that used input data for SAP2000 software.

Table 2: 20 earthquake ground motions records

| No. | Earthquake Name | Year | Station | Component | Data Source | PGA (g) |
|---|---|---|---|---|---|---|
| 1 | Anza (Horse Cany) | 1980 | 5160 | Azf225 | USGS | 0.065 |
| 2 | Chalfant | 1986 | 54428 | C-Zak270 | CDMG | 0.143 |
| 3 | Coalinga | 1983 | 46t04 | G-Chp000 | CDMG | 0.023 |
| 4 | Coyote | 1979 | 47379 | G01230 | CDMG | 0.103 |
| 5 | Helena Montana | 1935 | 2022 | A-Hmc180 | - | 0.150 |
| 6 | Hollister | 1986 | 47189 | D-Sg3205 | CDMG | 0.044 |
| 7 | Hollister | 1974 | 47379 | A-G01157 | CDMG | 0.105 |
| 8 | Imperial Valley | 1940 | 117 | I-Elc180 | USGS | 0.313 |
| 9 | Imperial Valley | 1979 | 5154 | H-Ecc002 | CDMG | 0.213 |
| 10 | Kobe | 1995 | 0Kjma | Kjm000 | - | 0.821 |
| 11 | Kocaeli | 1999 | Duzce | Dzc180 | ERD | 0.312 |
| 12 | Kocaeli | 1999 | Izmit | Izt180 | ERD | 0.152 |
| 13 | Landers | 1992 | Lucerne | Lcn275 | SCE | 0.721 |
| 14 | Livermore | 1980 | 57134 | A-Srm070 | CDMG | 0.058 |
| 15 | Mammoth Lakes | 1980 | 35 Long Valley Fire Sta | D-Xlv000 | USC | 0.026 |
| 16 | Morgan Hill | 1984 | 47379 | G01320 | CDMG | 0.098 |
| 17 | Parkfield | 1966 | 1013 | C02065 | CDMG | 0.476 |
| 18 | Bishop(Round Valley) | 1984 | 1661 | Mcg270 | USGS | 0.088 |
| 19 | Superstition Hills(B) | 1987 | El Centro 01335 | B-Icc000 | CDMG | 0.358 |
| 20 | Westmoreland | 1981 | 724 | Nil000 | CDMG | 0.105 |

Nonlinear dynamic time history analysis was performed to assess the seismic performance of the structures. It is more suitable to evaluate the damage level by measuring the peak displacements of the structural elements during the simulation. The inter-storey drift ratio (ISDR), i.e. the relative peak displacement between two consecutive floors, is a

widely-used indicator to measure the behaviour of the structures [18].

Most of building codes and computer softwares in order to simplification of elements nonlinear behaviour under earthquake loads used multiline models. According to Inel and Ozmen [8], content of this multiline model is variable and depend on element type, material properties, longitudinal and shear bars of concrete element and axial force. After analysis of structure based on selected earthquake acceleration time history records, structure displacements at joints are obtained. As regards storey displacement is important then derivate from model analysis, displacement of storey master joints. This displacement is absolute and converts to relative displacement and Drift of stories with following equations. For building structures, inter-storey drift ratio $\delta_i$, between i, i-1 stories, obtained by this equation.

$$\delta_i = \left( \frac{\Delta_i - \Delta_{i-1}}{h_i} \right) \tag{1}$$

$h_i$, is height between i, i-1 stories and $\Delta$, is the displacement of stories. Maximum inter-storey drift ratio $\delta_{max}$ expressed as following equation:

$$ISD_{\max\%} = Max(\delta_1, \delta_2, ..., \delta_n) \tag{2}$$

Max() is a function that determinate maximum content and n is the summery of all storey numbers [10]. In this study all of processing and calculation of $ISD_{max\%}$ was coding by Compaq Visual FORTRAN Ver.6. Homogenised Reinforced Concrete damage scale (HRC scale) used for development of fragility curves.

After creating a database of damage state versus peak ground acceleration for each model, the next step followed was to calculate cumulative distribution functions by dividing the number of data points that are in or exceed a particular damage state by the number of data points of the whole sample as proposed by [19]. This step is presented in Eq. (3)

$$f_i = \frac{n_i}{N} \tag{3}$$

Where, $f_i$ = cumulative distribution function data points, mi = number of data points that are in or exceed a particular damage state, and N = number of data points of the whole sample. With this information lognormal functions with two parameters (log-median and log-standard deviation) were fitted and fragility curves developed.

$$P[d >= DI | PGA] = \Phi\left( \frac{\ln(PGA) - \mu_{\ln}}{\sigma_{\ln}} \right) \tag{4}$$

Where, $\mu_{ln}$ and $\sigma_{ln}$ are median and standard deviation of ln(PGA). In fact, P function is probability of reaching of exceeding a specific damage state in a given PGA. To calibrate

this equation, the value of $\mu_{ln}$ and $\sigma_{ln}$ must be estimated [1]. These parameters are required to develop the cumulative normal distribution function.

According to FEMA-58-1 [4] engineering judgment can be used to fitting the cumulative normal distribution curve. In other words, the most adaptive curves are fitting by regressing. The parameters of fragility curves are collected in Table 3.

Table 3: The fragility curves parameters of analysed models

| Model Type | 5-storey model | | 8-Storey Model | |
|---|---|---|---|---|
| Damage State | $\mu_{ln}$ | $\sigma_{ln}$ | $\mu_{ln}$ | $\sigma_{ln}$ |
| None | 0.01 | 1.20 | 0.01 | 1.20 |
| Slight | 0.10 | 1.20 | 0.02 | 1.20 |
| Light | 0.15 | 1.20 | 0.07 | 1.20 |
| Moderate | 0.60 | 1.20 | 0.30 | 1.20 |
| Extensive | 1.70 | 1.20 | 1.30 | 1.20 |
| Partial collapse | 5.00 | 1.20 | 2.80 | 1.20 |
| Collapse | 10.00 | 1.2 | 5.00 | 1.20 |

The probability reaching or exceeding each damage states for 5 stories building at all PGA is summarized in Table 4. For example when PGA=0.4g, probability of reaching or exceeding moderate state is 50%. These values are fragility curves data points that presented by bar chart in Fig. 3. The fitted fragility curves for HRC each damage state is presented in Fig. 4.

Table 4: Data points of cumulative distribution function (the probability of reaching or exceeding damage state HRC) 5 stories building

| PGA | None | Slight | Light | Moderate | Extensive | Partial Collapse | Collapse |
|---|---|---|---|---|---|---|---|
| 0.10 | 1.00 | 0.50 | 0.50 | 0.05 | 0.00 | 0.00 | 0.00 |
| 0.20 | 1.00 | 0.75 | 0.60 | 0.25 | 0.00 | 0.00 | 0.00 |
| 0.30 | 1.00 | 0.85 | 0.65 | 0.40 | 0.05 | 0.00 | 0.00 |
| 0.40 | 1.00 | 0.90 | 0.80 | 0.50 | 0.05 | 0.00 | 0.00 |
| 0.50 | 1.00 | 0.90 | 0.85 | 0.50 | 0.15 | 0.00 | 0.00 |
| 0.60 | 1.00 | 0.95 | 0.90 | 0.50 | 0.15 | 0.00 | 0.00 |
| 0.70 | 1.00 | 0.95 | 0.90 | 0.50 | 0.25 | 0.05 | 0.00 |
| 0.80 | 1.00 | 0.95 | 0.90 | 0.50 | 0.30 | 0.05 | 0.00 |
| 0.90 | 1.00 | 0.95 | 0.90 | 0.65 | 0.35 | 0.05 | 0.00 |
| 1.00 | 1.00 | 0.95 | 0.90 | 0.65 | 0.35 | 0.05 | 0.00 |
| 1.10 | 1.00 | 0.95 | 0.90 | 0.65 | 0.35 | 0.10 | 0.05 |
| 1.20 | 1.00 | 0.95 | 0.95 | 0.70 | 0.40 | 0.15 | 0.05 |
| 1.30 | 1.00 | 1.00 | 0.95 | 0.70 | 0.40 | 0.15 | 0.05 |
| 1.40 | 1.00 | 1.00 | 0.95 | 0.80 | 0.45 | 0.15 | 0.05 |
| 1.50 | 1.00 | 1.00 | 0.95 | 0.80 | 0.50 | 0.20 | 0.05 |

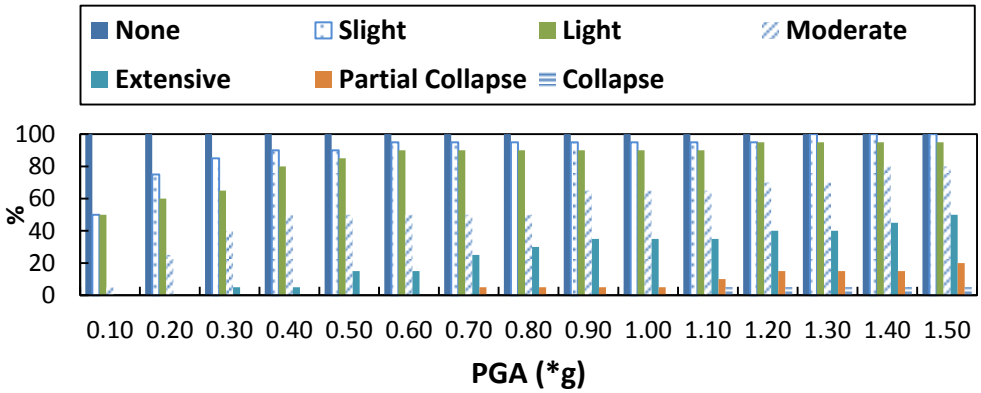


Figure 3. Data points of cumulative distribution function (the probability of reaching or exceeding damage state HRC) 5 stories building

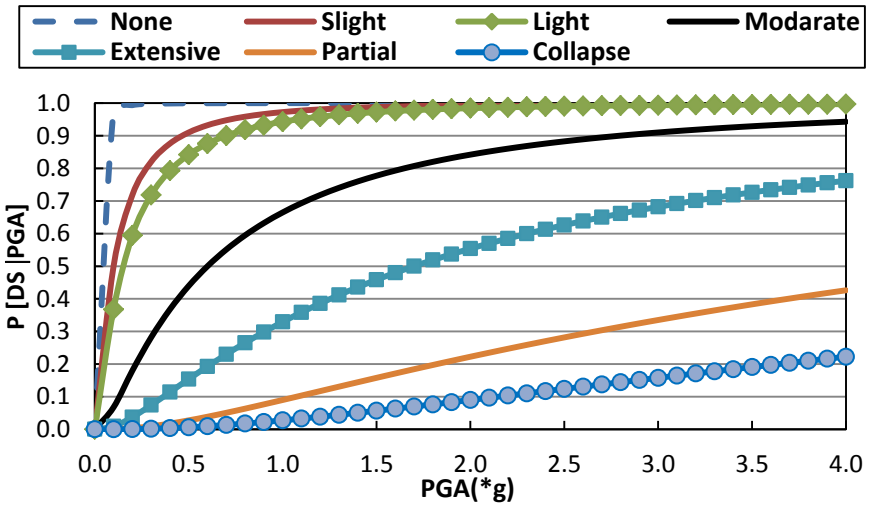


Figure 4. The fitted fragility curves for HRC each damage state for 5-storey building

The probability reaching or exceeding each damage states for 8 stories building at all PGA is summarized in Table 5. For example when PGA=0.5g, probability of reaching or exceeding Extensive state is 25%. The fitted fragility curves for HRC each damage state is presented in Fig. 5.

Table 5: Data points of cumulative distribution function (the probability of reaching or exceeding damage state HRC) 8 stories building

| PGA | None | Slight | Light | Moderate | Extensive | Partial Collapse | Collapse |
|---|---|---|---|---|---|---|---|
| 0.10 | 1.00 | 0.90 | 0.55 | 0.20 | 0.00 | 0.00 | 0.00 |
| 0.20 | 1.00 | 0.95 | 0.90 | 0.40 | 0.00 | 0.00 | 0.00 |
| 0.30 | 1.00 | 1.00 | 0.90 | 0.45 | 0.10 | 0.00 | 0.00 |
| 0.40 | 1.00 | 1.00 | 0.90 | 0.45 | 0.15 | 0.00 | 0.00 |

| | | | | | | | |
|---|---|---|---|---|---|---|---|
| 0.50 | 1.00 | 1.00 | 0.90 | 0.50 | 0.25 | 0.00 | 0.00 |
| 0.60 | 1.00 | 1.00 | 0.95 | 0.55 | 0.30 | 0.00 | 0.00 |
| 0.70 | 1.00 | 1.00 | 0.95 | 0.70 | 0.40 | 0.10 | 0.00 |
| 0.80 | 1.00 | 1.00 | 0.95 | 0.80 | 0.40 | 0.10 | 0.00 |
| 0.90 | 1.00 | 1.00 | 1.00 | 0.90 | 0.40 | 0.15 | 0.00 |
| 1.00 | 1.00 | 1.00 | 1.00 | 0.90 | 0.40 | 0.20 | 0.10 |
| 1.10 | 1.00 | 1.00 | 1.00 | 0.90 | 0.40 | 0.25 | 0.10 |
| 1.20 | 1.00 | 1.00 | 1.00 | 0.90 | 0.40 | 0.25 | 0.10 |
| 1.30 | 1.00 | 1.00 | 1.00 | 0.90 | 0.45 | 0.25 | 0.10 |
| 1.40 | 1.00 | 1.00 | 1.00 | 0.90 | 0.45 | 0.30 | 0.15 |
| 1.50 | 1.00 | 1.00 | 1.00 | 0.90 | 0.45 | 0.30 | 0.15 |

Recognition of structures properties including period is an important criteria. The structure height or the number of stories has directly effect on main period of building. Therefore, to investigate the probability of buildings damage, their height or number of stories was compared. Thus, the fragility curves of two models are combined together for each damage state. These curves are showed in Fig. 6.

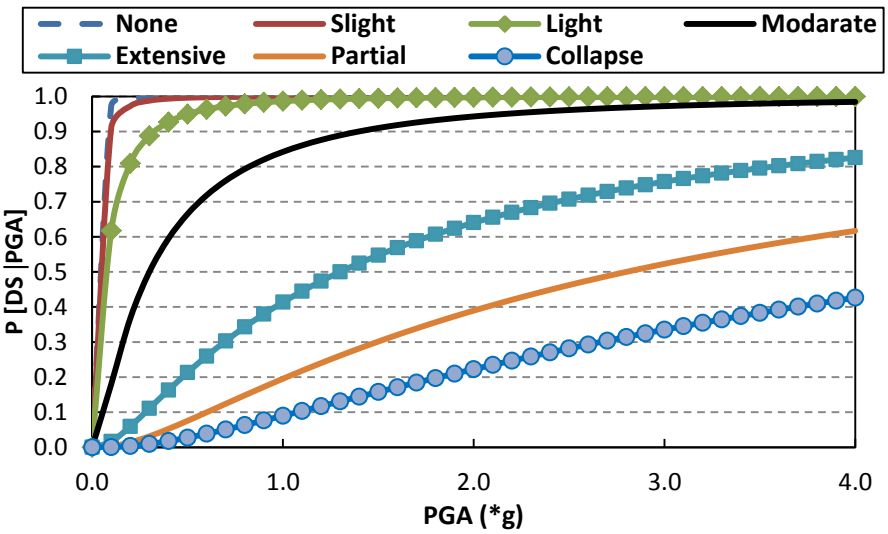


Figure 5. The fitted fragility curves for HRC each damage state for 8-storey building

## 3. CONCLUSIONS

To investigate the structural behavior, recognition of the structure modal properties such as period is more important. These properties are different in variety structure modes. Despite the importance of these properties in the main mode of structure, other modes consideration is important and increases the computational accuracy. In this section SAP2000 model results has been applied to conclude by using of modal properties based on structure period in number 1 to 8 modes. In Table 6, the period, Frequency and Eigenvalue of each models are presented.

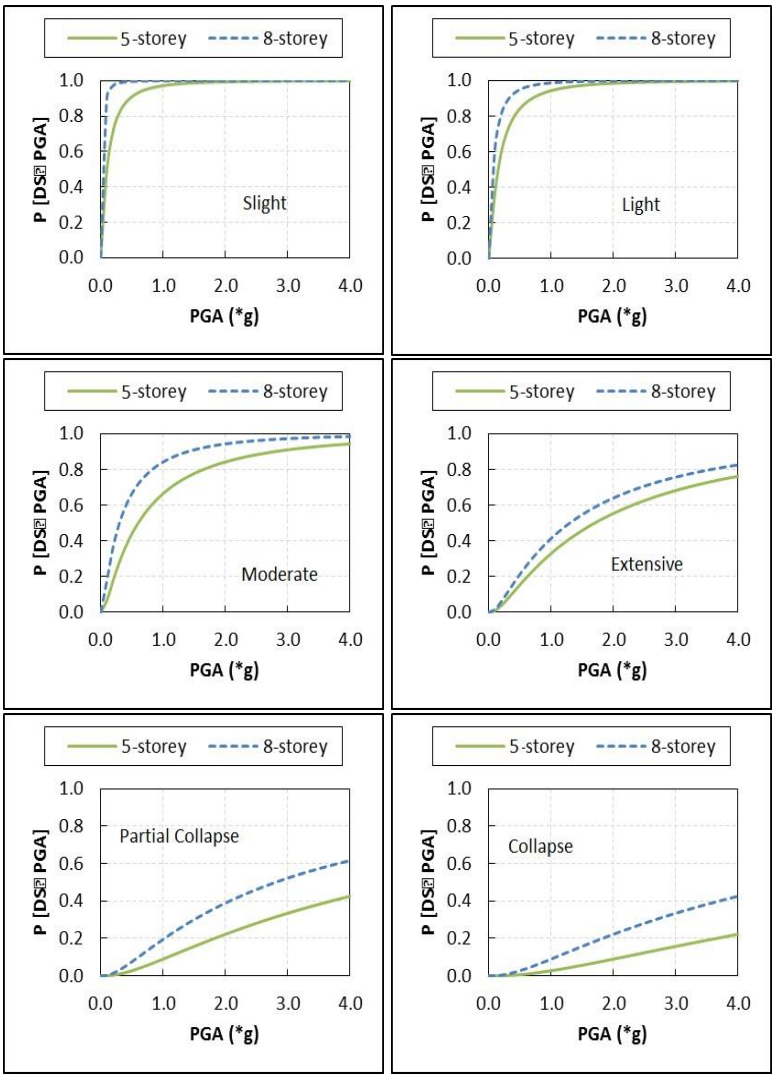


Figure 6. The fitted fragility curves for HRC each damage state for 8-storey building

Table 6: Modal properties of structures

| Model | 5-storey | | | 8-storey | | |
|---|---|---|---|---|---|---|
| Mode no. Unit less | Period Sec | Frequency Cyc/sec | Eigenvalue $rad^2/sec^2$ | Period Sec | Frequency Cyc/sec | Eigenvalue $rad^2/sec^2$ |
| 1 | 0.85 | 1.172 | 54.225 | 1.11 | 0.90 | 31.93 |
| 2 | 0.77 | 1.2964 | 66.355 | 1.08 | 0.93 | 33.798 |
| 3 | 0.69 | 1.4584 | 83.969 | 0.98 | 1.02 | 41.472 |
| 4 | 0.30 | 3.3613 | 446.03 | 0.37 | 2.67 | 281.91 |
| 5 | 0.26 | 3.7919 | 567.63 | 0.37 | 2.73 | 295.8 |
| 6 | 0.24 | 4.1771 | 688.83 | 0.33 | 3.04 | 364.57 |
| 7 | 0.16 | 6.2052 | 1520.1 | 0.21 | 4.66 | 857.27 |
| 8 | 0.14 | 7.1133 | 1997.6 | 0.21 | 4.79 | 905.01 |

Consideration the main period of models structure shows that in these models the period increased by increasing the structures elevation. This increasing effect on fragility curves that presented in Fig. 6. Evaluation of fragility curves of two models, 5 and 8 stories, show the probability that a structure will reach or exceed moderate damage state in PGA = 0.35g are 33% and 55%, respectively. This damage state is named as “life safe” damage state.

According to the Iranian Standard No. 2800, the design based acceleration of Tabriz region is determines as 0.35g. Thus, it is important to consider the probability of reaching or exceeding each damage states in mentioned acceleration. These results have been obtained from the fragility curves of the modeled structures and presented in Table 7.

Table 7: The probability of reaching different damage states in design based acceleration 0.35g

| Damage State / Model Type | None | Slight | Light | Moderate | Extensive | Partial Collapse | Collapse |
|---|---|---|---|---|---|---|---|
| 5-Storey | 100 | 85 | 76 | 33 | 10 | 2 | 0 |
| 8-Storey | 100 | 99 | 91 | 55 | 14 | 4 | 1 |

Comparison of fragility curves of the two models indicates that the probability reach or exceed each damage states for 5 stories building at all PGA is significantly lower than the probability for 8 stories building. In other words, 8 stories model is more vulnerable than other model. This difference is observed about 10%-20% in PGA < 0.1g. For example, in moderate damage state and in PGA = 0. 5g, difference between two models is 22%.The probability in Moderate damage state and in PGA = 1.0g are 66% and 84% for 5 story and 8 stories building, respectively and difference is about 18%. Zare et al [20] expressed the Peak ground acceleration in recent Varzeghan earthquake (2012) in vicinity of Tabriz, more than $0.5g$.

In partial collapse and collapse damage state, the buildings completely damaged and must be destroyed and rebuilt. Therefore this condition is more consequential in crisis management planning. Thus in two simulated models, these probabilities in PGA = 0.5g are extracted and evaluated. The results are presented in Table 8.

Table 8: The probability of reaching different damage states in design based acceleration 0.5g

| Damage state / Model | Partial Collapse | Collapse |
|---|---|---|
| 5 stories model | 3.0% | 0.1% |
| 8 stories model | 8.0% | 3.0% |

As shown in Table 7, collapse probability is significant for 8 stories building. Since, in this study area, there are many building in this class, their assessment and retrofitting is important problem.

## REFERENCES


1. Baker JW. Efficient Analytical Fragility Function Fitting Using Dynamic Structural Analysis, *Earthquake Spectra*, (In Press), 2014.
2. Division of the State Architect Earthquake Hazard Mitigation Technology: *Application Guidelines and Recommendations*, Sacramento, 1996.
3. Derecho AT, Kianoush MR. Seismic Design of Reinforced Concrete Structures, *The Seismic Design Handbook*, 2nd Edition, 465-558, 2001.
4. FEMA-P-58-1, Seismic Performance Assessment of Buildings, Vol.1-Metodology, 2012.
5. Ferritto JM. An economic analysis of earthquake design levels for new concrete construction, *Department of the Navy Civil Engineering Laboratory Report No. N-1671*, Port Hueneme, 1983.
6. Haselton CB, Liel AB, Deierlein GG, Dean BS and Chou JH. Seismic collapse safety of reinforced concrete buildings: assessment of ductile moment frames, *Journal of Structural Engineering*, No. 4, **137**(2011) 481-91.
7. Hessami K, Pantosti D, Tabassi H, Shabanian E, Abbassi M, Feghhi K and Solaymani S. Pale earthquakes and slip rates of the North-Tabriz Fault, NW Iran: preliminary results, *Annals of Geophysics*, 2003, 46(5).
8. Inel M, Ozmen HB. Effects of plastic hinge properties in nonlinear analysis of reinforced concrete buildings, *Engineering Structures*, **28**(2006) 1494-1502.
9. Jalali A, Ohmachi T. Aspects of concrete dams response to near-field ground motions, *Proceeding of the World Conference on Earthquake Engineering*, Auckland, New Zealand, 30 January-3 February, 2000.
10. Jeonga SH, Elnashai AS. Probabilistic fragility analysis parameterized by fundamental response quantities, *Engineering Structures*, **29**(2007) 1238-51.
11. Kalkan ES, Kwong N. Evaluation of Fault-Normal/Fault-Parallel Directions Rotated Ground Motions for Response History Analysis of an Instrumented Six-Story Building, U.S. Geological Survey, Reston, Virginia, 2012.
12. Kircher CA, Nassar AA, Kustu O, Holmes WT. Development of Building Damage Functions for Earthquake Loss Estimation, *Earthquake Spectra*, No. 4, **13**(1997) 663-81.
13. Liel AB, Champion C. The Effect of Near-Fault Directivity on Building Seismic Collapse Risk, Final Report to U.S. Geological Survey, 2012.
14. PEER SPD (Structural Performance Database). http://nisee.berkeley.edu/spd/. Web page, 2014.
15. Rossetto T, Elnashai A. A new analytical procedure for the derivation of displacement-based vulnerability curves for populations of RC structures, *Engineering Structures*, **27**(2005) 397-409.
16. Rossetto T, Elnashai A. Derivation of vulnerability functions for European-type RC structures based on observational data, *Engineering Structures*, **25**(2003) 1241-63.

17. SAP2000 Manual, *Computers and Structures*, Inc. Berkeley, California, USA, 2015.
18. Seyedi DM, Gehl P, Douglas J, Davenne L, Mezher N, Ghavamian S. Development of seismic fragility surfaces for reinforced concrete buildings by means of nonlinear time-history analysis, *Earthquake Engineering and Structural Dynamics*, **2010**(39) 91-108
19. Vafaie J, Taghikhany T and Tehranizadeh M. Near field effect on horizontal equal-hazard spectrum of Tabriz city in north-west of Iran, *International Journal of Civil Engineering*, No. 1, **9**(2011) 49-56.
20. Zare et al. Preliminary Earthquake Report-Varzeghan, East Azerbaijan, Iran, 2012-08-11, *International Institute of Earthquake Engineering and Seismology*, 2012.